Table XI. Final Fractional Coordinates for $[LuCl_3(EO3)]$

atom	x/a	y/b	z/c	U(eqv)[a]
Lu	0.5000	-0.07703 (3)	0.2500	0.006
Cl(1)	0.5000	0.0950 (2)	0.2500	0.014
Cl(2)	0.7499 (2)	-0.0981 (1)	0.4051 (1)	0.013
O(1)	0.3012 (6)	-0.0459 (3)	0.3978 (5)	0.014
O(2)	0.3847 (6)	-0.2088 (4)	0.3379 (4)	0.011
C(1)	0.226 (1)	-0.1187 (5)	0.4718 (7)	(iso)
C(2)	0.2118 (9)	-0.1982 (5)	0.3917 (7)	0.011
C(3)	0.408 (1)	-0.2942 (5)	0.2723 (7)	0.016
H(1)[O(1)]	0.321	-0.004	0.440	(iso)

[a] $U(eqv)$ is equal to $(U_{11} + U_{22} + U_{33})/3$.

= 5.5 Å^2) in the final refinement. C(1) could not be refined anisotropically. The final positional parameters are given in Table XI.

Acknowledgment. We wish to thank the Illinois Department of Commerce and Community Affairs and the donors of the Petroleum Research Fund, administered by the American Chemical Society, for support of this work. The U.S. National Science Foundation's Chemical Instrumentation Program provided funds used to purchase the diffractometer.

Registry No. $[DyCl_3(EO3)]$·18-crown-6, 111976-41-1; $[YCl_3(EO3)]$·18-crown-6, 111976-39-7; $[Nd(OH_2)_5(EO3)]Cl_3$, 111976-45-5; $[Eu(OH_2)_5(EO3)]Cl_3$, 111976-44-4; $[Gd(OH_2)_5(EO3)]Cl_3$, 111976-43-3; $[Dy(OH_2)_5(EO3)]Cl_3$, 111997-42-3; $[Y(OH_2)_5(EO3)]Cl_3$, 111976-42-2; $[HoCl_3(EO3)]\cdot CH_3CN$, 111976-37-5; $[LuCl_3(EO3)]\cdot CH_3CN$, 111976-35-3; $[ErCl_3(EO3)]$·OHMe, 111976-34-2; $[YbCl_3(EO3)]$·OHMe, 111976-32-0; $[LuCl_3(EO3)]$, 111976-30-8; $[Sm(OH_2)_5(EO3)]Cl_3$, 111976-46-6.

Supplementary Material Available: Tables SI-SXLI, listing hydrogen atom coordinates and thermal parameters for all complexes, fractional coordinates for those complexes not in the text, hydrogen bond contact geometries, bond distances and angles for the 18-crown-6 complexes, and representative least-squares plane results (27 pages); Tables SXLII-SLIV, listing observed and calculated structure factors or structure factor amplitudes for all complexes (93 pages). Ordering information is given on any current masthead page.

Contribution from the Laboratoire de Spectrochimie des Elêments de Transition, UA No. 420, and Laboratoire de Chimie Physique des Matêriaux Amorphes, UA No. 1104, Universitê de Paris Sud, 91405 Orsay, France, Department of Chemistry, University of Bergen, 5007 Bergen, Norway, and Departamento de Quimica Inorganica, Facultad de Ciencias Quimicas, Burjassot, Valencia, Spain

Phase Transition and Exchange Interaction in (μ-Carbonato)bis[(*N*,*N*,*N*′,*N*″,*N*″-pentaethyldiethylenetriamine)copper(II)] Diperchlorate

Jorunn Sletten,*[1a] Hakon Hope,[1a,e] Miguel Julve,[1b] Olivier Kahn,*[1c] Michel Verdaguer,[1c] and Ary Dworkin[1d]

Received August 6, 1987

The title compound, $[(Cu(petdien))_2(CO_3)](ClO_4)_2$, has been synthesized and its crystal structure has been determined at 294 K (high-temperature (HT) modification) and 92 K (low-temperature (LT) modification). Crystal data: for HT, orthorhombic system, space group $Cmc2_1$, a = 18.610 (3) Å, b = 15.449 (3) Å, c = 14.499 (7) Å, Z = 4; for LT, monoclinic system, space group $P2_1$, a = 12.037 (1) Å, b = 13.145 (3) Å, c = 12.519 (2) Å, β = 96.85 (1)°, Z = 2. The phase transition between the HT and the LT forms occurs around 208 K. For the two modifications, the structure consists of dinuclear cations and noncoordinated perchlorate ions. Copper(II) is located in distorted-trigonal-bipyramid surroundings. An oxygen atom of the carbonato bridge is bound to the two copper atoms of the dinuclear unit; each of the other two oxygen atoms is bound to only one copper atom. In the LT modification, the Cu-O distances involving the doubly coordinated oxygen atom are in average 0.06 Å shorter than in the HT modification, but the average of the metal-ligand bond lengths remains unchanged. The magnetic properties have been investigated in the 300-20 K temperature range. The molar magnetic susceptibility exhibits a break at T_c, with an hysteresis of about 3 K. The S-T energy gap has been found to be J = -207 (1) cm^{-1} above T_c and J = -215 (1) cm^{-1} below T_c. The enthalpy and entropy variations associated with the phase transition have been determined by differential scanning calorimetry measurements and found to be ΔH = 3.17 (4) kJ mol^{-1} and ΔS = 15.1 (2) J mol^{-1} K^{-1}.

Introduction

In several cases, a temperature dependence of the exchange parameter J in an exchange-coupled system has been postulated or even demonstrated.[2-5] The most likely origin of this phenomenon is a change of the geometrical structure of the system versus the temperature. This change may be gradual, without phase transition, or abrupt. In this latter case, it is associated with a crystallographic phase transition. A gradual change may occur when the bridging network has a specific nonrigidity. One of us called this phenomenon the exchange elasticity and reported such a situation in copper(II) dinuclear compounds resulting from the inclusion of the two metallic sites into intramolecular cavities containing two cation binding subunits.[4] Another convincing example of exchange elasticity due to the flexibility of the bridges is provided by hydrogen-bonded copper dimers.[2]

The solid-state physicists have often described small deviations of the magnetic properties from the predictions of the Heisenberg spin Hamiltonian in terms of exchange striction.[6-8] Basically, the exchange striction results from a modulation of J due to the molecular vibrations. A nice example of temperature dependence of J in a Cr(III) dinuclear complex, attributed to exchange striction, has been given by Güdel and Furrer[3]. The relative energies of the low-lying states in that case have been accurately determined by inelastic neutron scattering. A temperature dependence of J could also arise from the fact that the vibrational levels associated with a given low-lying electronic state depend on this state.[9]

To be complete, it is fair to say that in some works to which we will not refer, the claimed temperature dependence of J has its origin in the uncertainties of the experimental data. Such an

(1) (a) University of Bergen. (b) Facultad de Ciencias Quimicas Valencia. (c) UA No. 420, Universitê de Paris Sud. (d) UA No. 1104, Universitê de Paris Sud. (e) On leave from the University of California, Davis, CA 95616.
(2) Duggan, D. M.; Hendrickson, D. N. *Inorg. Chem.* **1974**, *13*, 2929.
(3) Güdel, H. U.; Furrer, A. *Mol. Phys.* **1977**, *33*, 1335.
(4) Kahn, O.; Morgenstern-Badarau, I.; Audière, J. P.; Lehn, J. M.; Sullivan, S. A. *J. Am. Chem. Soc.* **1980**, *102*, 5935.
(5) Mikuriya, M.; Okawa, H.; Kida, S. *Bull. Chem. Soc. Jpn.* **1981**, *54*, 2979.
(6) Kennedy, T. A.; Choh, S. H.; Seidel, G. *Phys. Rev. B: Solid State* **1970**, *2*, 3645.
(7) Lines, M. E. *Solid State Commun.* **1972**, *11*, 1615.
(8) Katriel, J.; Kahn, O. *Phys. Lett. A* **1976**, *55A*, 439.
(9) Martin, R. L. *Inorg. Chem.* **1966**, *5*, 2065.

0020-1669/88/1327-0542$01.50/0

artifact may be obtained when the displayed temperature deviates from the actual temperature of the sample.

The reports on abrupt variations of J in coupled systems, due to a phase transition, are very rare.[5] In fact, we are not aware of any investigation of that sort concerning polymetallic molecular units, for which both the low-temperature (LT) and high-temperature (HT) crystal structures have been solved. On the other hand, a few studies of this kind dealing with one-dimensional magnetic systems have appeared, in connection with the problem of the spin Peierls transition.[10-12]

Several crystallographic and magnetic studies concerning mononuclear complexes in which a spin transition takes place have been published. In that case, the crystallographic phase transition accompanies the electronic bistability, and the magnetic properties, at the temperature of the transition, are totally modified.[13-15] Otherwise, when a transition occurs in a mononuclear molecular compound without modification of the nature of the ground state, its influence on the magnetic properties is very weak. Indeed, only the g factor may be slightly modified, owing to the change in the surroundings of the metal center. In contrast, with a dinuclear compound, even a small change in the geometry of the bridging network may lead to a significant variation of J and hence to a well-pronounced discontinuity in the magnetic susceptibility curve.[16,17]

In the course of our work on dinuclear copper(II) compounds with extended bridging ligands,[17] we have obtained the compound (μ-carbonato)bis[(N,N,N',N'',N''-pentaethyldiethylenetriamine]copper(II)) diperchlorate, hereafter $[(Cu(petdien))_2(CO_3)](ClO_4)_2$. This compound presents a phase transition around 208 K, and this paper is devoted to a thorough investigation of this transition and of its influence on the magnetic properties. We will successively describe the synthesis of the compound, its molecular and crystal structure both above and below the transition, and its magnetic and thermodynamic properties.

Experimental Section

Synthesis. A 4-mmol sample of sodium carbonate dissolved in a minimum amount of water was added with stirring to an aqueous solution of 10 mmol of copper(II) perchlorate and 10 mmol of petdien (N,N,N',N'',N''-pentaethyldiethylenetriamine). The total volume was 100 mL. The solution was filtered, and pyramidal dark blue crystals of the title compound were obtained by slow evaporation of the solution at room temperature. Well-shaped large single crystals were obtained by recrystallization from dilute warm aqueous solution.

Anal. Calcd for $C_{29}H_{36}N_6O_{11}Cl_2Cu_2$: C, 39.93; H, 7.57; N, 9.63; Cl, 8.13; Cu, 14.57. Found: C, 40.03; H, 7.47; N, 9.72; Cl, 8.16; Cu, 14.40.

Crystallographic Data Collection. Data were first collected at room temperature, 294 K, for the high-temperature modification (HT 1). Later, a set of data was collected at 236 K (HT 2) on another crystal. Lowering of the temperature caused the mosaic spread of the crystal to increase. The first several attempts at obtaining a single crystal of the low-temperature modification failed. Shock cooling as well as fairly slow cooling was tried. Finally, a slow decrease of the temperature from 294 to 205 K over a period of 3–4 h proved successful. First, data of the low-temperature modification were collected at 205.5 K (LT 1). Later another crystal was brought through the phase transition and cooled further down to 92 K, and a new data set (LT 2) was collected. Cell dimensions at 294 K were determined from measurements of diffractometer setting angles for 25 reflections with θ values in the region 9–17°. At 92 K, 23 reflections in the region 9–20° were used. Cell dimensions were furthermore monitored during cooling for some crystals. For these measurements the number of reflections used varied from 8 to 25. Table V summarizes the variation in cell dimensions. All measurements were done on a CAD-4 diffractometer equipped with a liquid-nitrogen cooling device, which has been modified for increased stability and lower temperature at the crystal site by H. H. In all four data collections, three reference reflections were monitored. For the LT data sets a slow but significant deterioration was observed as the intensities of the reference reflections decreased by 3–5%. No significant decrease was observed for the HT data sets. The usual corrections for Lorentz and polarization effects were done. In addition the data were corrected for absorption: HT 1 by the Gaussian integration method; HT 2 and LT by an empirical method during the refinement.[18] The crystals used for collecting HT 2 and LT 1 were both ruined in attempts on further cooling, and the crystal used for collecting LT 2 fractured as the temperature was raised after data collection. Crystal faces had not been indexed before data collections. Hence, for these data sets an empirical absorption correction was used. Information concerning conditions for the data collections are summarized in Table I for HT 1 and LT 2.

Table I. Information Concerning the Crystallographic Data Collection and Refinement Conditions for $[(Cu(petdien))_2(CO_3)](ClO_4)_2$ ($Cu_2Cl_2C_{23}H_{66}N_6O_{11}$)[a]

	modification	
	HT	LT
fw	872.87	872.87
space group	$Cmc2_1$ (No. 36)	$P2_1$ (No. 4)
temp at cryst, K	294	92
unit cell		
a, Å	18.610 (3)	12.037 (1)
b, Å	15.449 (3)	13.145 (3)
c, Å	14.499 (7)	12.519 (2)
β, deg		96.85 (1)
V, Å^3	4168 (3)	1967 (1)
Z	4	2
D_{exptl}, g cm^{-3}	1.391	1.474
μ(Mo Kα), cm^{-1}	12.07	12.79
cryst size, mm	0.63 × 0.41 × 0.38	0.35 × 0.31 × 0.15
instrument	CAD-4	CAD-4
scan type	ω	ω
scan range ($\Delta\omega$), deg	0.65 + 0.35 (tan θ)	1.00 + 0.35(tan θ)
scan speed, deg/min	5	4
radiation	Mo Kα (λ = 0.71073 Å)	Mo Kα (λ = 0.71073 Å)
monochromator	graphite	graphite
max 2θ, deg	56	56
no. of indep reflcns measd	2672	4949
no. obsd reflcns (NO)	1571	3983
limit of obsd reflcns	$F_o > 2\sigma_F$	$F_o > 3\sigma_F$
no. of variables refined (NV)	241	452
extinction coeff	7.96 × 10^{-8}	4.45 × 10^{-8}
agreement factors[b]		
R	0.058	0.043
R_w	0.050	0.042
s	2.20	1.69

[a] Atomic scattering factors and programs used are those of ref 19 and 20. [b] Agreement factors are defined as follows: $R = \sum||F_o| - |F_c||/\sum|F_o|$; $R_w = [\sum w(|F_o| - |F_c|)^2/\sum w|F_o|^2]^{1/2}$; $s = [\sum w(|F_o| - |F_c|)^2/(NO - NV)]^{1/2}$. The weighting scheme is defined by $w = 1/\sigma_F^2$; $\sigma_F = \sigma_I[I(Lp)]^{-1/2}$. $\sigma_I = [\sigma_c^2 + (0.02N_{net})^2]^{1/2}$.

Solution and Refinement. (a) HT Structure. Systematic extinctions showed that the space group might be $Ama2$, $Cmc2_1$, or $Cmcm$. The intensity distribution was clearly acentric; hence, the two former space groups are possible. Solution of the structure by direct methods was attempted in both space groups. No possible solution was found in $Ama2$. The structure was solved, with some difficulty, in space group $Cmc2_1$. From several of the E maps, Cu positions consistent with the largest Patterson peaks could be located. None of the maps, however, revealed the copper coordination clearly. A Fourier map based on the phasing by

(10) Hall, J. W.; Marsh, W. E.; Weller, R. R.; Hatfield, W. E. *Inorg. Chem.* **1981**, *20*, 1033.
(11) Wolthuis, A. J.; Huiskamp, W. J.; de Jongh, L. J.; Reedijk, J. *Physica B+C (Amsterdam)* **1985**, *133B+C*, 161.
(12) de Jongh, L. J.; de Groot, H. J. M.; Reedijk, J. *J. Appl. Phys.* **1982**, *53*, 8027.
(13) Gütlich, P. *Struct. Bonding (Berlin)* **1981**, *44*, 83 and references therein.
(14) Thuery, P.; Zarembowitch, J.; Michalowicz, A.; Kahn, O. *Inorg. Chem.* **1987**, *26*, 851 and references therein.
(15) König, E.; Ritter, G.; Kulshreshtha, K. S. *Chem. Rev.* **1985**, *85*, 219 and references therein.
(16) Crawford, W. H.; Richardson, H. W.; Wasson, J. R.; Hodgson, D. J.; Hatfield, W. E. *Inorg. Chem.* **1976**, *15*, 2107.
(17) Kahn, O. *Angew. Chem., Int. Ed. Engl.* **1985**, *24*, 834 and references therein.
(18) Walker, N.; Stuart, D. *Acta Crystallogr., Sect. A: Found. Crystallogr.* **1983**, *A39*, 159.
(19) Cromer, D. T.; Waber, J. T. *International Tables for X-ray Crystallography*; Kynoch: Birmingham, England, 1974; Vol. IV, p 99 (Table 2.2 B).
(20) Frenz, B. A. *The SDP-User's Guide*; Enraf-Nonius: Delft, The Netherlands, 1983.

Table II. Parameters of Non-Hydrogen Atoms for $[(Cu(petdien))_2(CO_3)](ClO_4)_2$

atom	x	y	z	B_{eq},[a] Å^2	atom	x	y	z	B_{eq},[a] Å^2
				(a) HT Modification (294 K)					
Cu1	0.500	0.19166 (8)	0.237	5.90 (3)	C3	0.4389 (8)	0.0299 (7)	0.2649 (9)	18.4 (5)
Cu2	0.500	0.42184 (8)	0.4384 (1)	5.68 (3)	C4	0.3426 (5)	0.2181 (5)	0.2529 (8)	8.2 (3)
Cl	0.3140 (1)	0.1277 (1)	0.5703 (2)	8.89 (7)	C5	0.2642 (6)	0.1951 (8)	0.251 (1)	14.7 (5)
O1	0.500	0.2916 (1)	0.3551 (5)	4.9 (2)	C6	0.3929 (7)	0.158 (1)	0.097 (1)	18.7 (5)
O2	0.500	0.3141 (4)	0.2053 (4)	5.4 (2)	C7	0.3877 (8)	0.2212 (9)	0.056 (1)	20.3 (5)
O3	0.500	0.4263 (4)	0.3037 (4)	4.8 (2)	C8	0.500	0.0920 (8)	0.4008 (9)	8.6 (4)
O4	0.2555 (4)	0.1015 (5)	0.6171 (7)	14.5 (3)	C9	0.500	0.000	0.454 (1)	12.1 (5)
O5	0.3713 (5)	0.1300 (8)	0.6242 (9)	24.1 (4)	C10	0.3751 (6)	0.4249 (8)	0.5514 (7)	12.8 (4)
O6	0.3066 (6)	0.2009 (5)	0.534 (1)	22.1 (4)	C11	0.4379 (8)	0.4311 (7)	0.6139 (7)	14.3 (5)
O7	0.3284 (6)	0.0678 (7)	0.506 (1)	22.1 (4)	C12	0.3485 (5)	0.4053 (7)	0.3971 (9)	11.6 (4)
N1	0.3946 (4)	0.1643 (5)	0.2037 (5)	8.5 (2)	C13	0.2661 (6)	0.4145 (9)	0.408 (1)	17.7 (6)
N2	0.500	0.0766 (6)	0.3000 (8)	9.5 (3)	C14	0.3855 (6)	0.5489 (7)	0.4530 (9)	13.1 (4)
N3	0.3932 (4)	0.4552 (4)	0.4573 (5)	7.6 (2)	C15	0.3983 (7)	0.5928 (8)	0.3716 (9)	13.9 (4)
N4	0.500	0.3913 (6)	0.5710 (7)	8.5 (3)	C16	0.500	0.2929 (7)	0.5807 (9)	7.8 (4)
C1	0.500	0.3445 (6)	0.2867 (6)	4.1 (2)	C17	0.500	0.250	0.6775 (9)	10.4 (5)
C2	0.3841 (6)	0.0728 (6)	0.239 (2)	19.9 (7)					
				(b) LT Modification (92 K)					
Cu1	0.19103 (5)	0.237	0.20544 (5)	1.38 (1)	C3A	−0.0400 (5)	0.2984 (6)	0.1559 (5)	2.7 (1)
Cu2	0.42456 (5)	0.45329 (6)	0.39848 (5)	1.17 (1)	C4	0.3788 (5)	0.2513 (5)	0.0674 (4)	2.2 (1)
Cl	0.3040 (1)	0.5800 (1)	−0.0619 (1)	1.91 (3)	C4A	0.0634 (4)	0.2713 (5)	0.3806 (5)	2.2 (1)
ClA	−0.0655 (1)	0.6100 (2)	0.3172 (1)	3.30 (4)	C5	0.4341 (6)	0.2370 (7)	−0.0347 (5)	4.4 (2)
O1	0.2980 (3)	0.3620 (3)	0.2910 (3)	1.13 (7)	C5A	−0.0421 (5)	0.2743 (7)	0.4362 (6)	4.3 (2)
O2	0.3113 (3)	0.1966 (3)	0.3157 (3)	1.38 (7)	C6	0.2579 (6)	0.0977 (5)	0.0414 (5)	3.4 (1)
O3	0.4257 (3)	0.3039 (3)	0.4185 (3)	1.03 (7)	C6A	0.0826 (6)	0.0918 (6)	0.3456 (5)	3.8 (1)
O4	0.3653 (4)	0.6206 (4)	−0.1430 (3)	2.9 (1)	C7	0.3384 (6)	0.0352 (5)	0.1160 (5)	2.9 (1)
O4A	−0.1375 (4)	0.6546 (5)	0.3875 (4)	4.2 (1)	C7A	0.0805 (6)	0.0044 (6)	0.2683 (6)	4.0 (2)
O5	0.2510 (4)	0.6618 (4)	−0.0108 (3)	3.3 (1)	C8	0.1030 (4)	0.4236 (4)	0.1183 (4)	1.2 (1)
O5A	−0.0198 (4)	0.6869 (6)	0.2545 (4)	5.5 (2)	C9	0.0245 (5)	0.4924 (5)	0.0483 (5)	2.0 (1)
O6	0.3790 (4)	0.5272 (4)	0.0172 (3)	3.0 (1)	C10	0.5793 (7)	0.5592 (6)	0.2946 (8)	9.6 (2)
O6A	0.0253 (4)	0.5581 (5)	0.3795 (4)	4.8 (1)	C10A	0.3109 (6)	0.6014 (5)	0.5113 (5)	2.7 (1)
O7	0.2197 (4)	0.5104 (4)	−0.1100 (4)	3.6 (1)	C11	0.4913 (5)	0.6261 (6)	0.2867 (6)	4.1 (2)
O7A	−0.1290 (4)	0.5407 (5)	0.2459 (4)	5.8 (1)	C11A	0.3902 (6)	0.6546 (5)	0.4453 (5)	3.2 (1)
N1	0.2630 (4)	0.2100 (4)	0.0637 (4)	2.0 (1)	C12	0.5610 (7)	0.3908 (7)	0.2373 (7)	8.9 (2)
N1A	0.0661 (4)	0.1924 (4)	0.2929 (4)	2.3 (1)	C12A	0.2514 (5)	0.4275 (5)	0.5441 (5)	2.4 (1)
N2	0.0714 (4)	0.3143 (4)	0.1144 (4)	1.40 (9)	C13	0.6579 (7)	0.3933 (7)	0.1665 (8)	10.5 (2)
N3	0.5720 (3)	0.4587 (4)	0.3286 (3)	1.50 (8)	C13A	0.1862 (6)	0.4482 (7)	0.6378 (5)	4.4 (2)
N3A	0.3494 (4)	0.4959 (4)	0.5355 (4)	1.85 (9)	C14	0.6692 (6)	0.434 (2)	0.3998 (7)	18.9 (5)
N4	0.3953 (4)	0.5953 (4)	0.3445 (4)	1.84 (9)	C14A	0.4323 (6)	0.4972 (5)	0.6341 (4)	2.4 (1)
C1	0.3467 (4)	0.2862 (1)	0.3426 (4)	0.9 (1)	C15	0.6962 (6)	0.4281 (6)	0.4990 (6)	4.1 (2)
C2	0.1886 (5)	0.2636 (5)	−0.0235 (4)	2.5 (1)	C15A	0.4651 (7)	0.3913 (5)	0.6734 (5)	3.2 (2)
C2A	−0.0362 (5)	0.1961 (5)	0.2129 (5)	3.0 (1)	C16	0.2893 (4)	0.6021 (4)	0.2702 (4)	1.5 (1)
C3	0.0703 (5)	0.2693 (5)	0.0054 (5)	2.6 (1)	C17	0.2507 (5)	0.7093 (5)	0.2399 (5)	2.6 (1)

[a] The temperature factors are given in the form of the isotropic equivalent thermal parameter: $B_{eq} = {}^4/_3\sum_i\sum_j\beta_{ij}\mathbf{a}_i\cdot\mathbf{a}_j$.

the Cu atoms yielded the bridging carbonato group and two of the N atoms, all located on the mirror plane. The remaining atoms were localized through a series of Fourier maps and partial refinement cycles. One reason for the slow phasing process may be the fact that a large fraction of the atoms are situated in special positions, on the crystallographic mirror plane. The subsequent refinement led to high thermal parameters, especially for some carbon atoms of the petdien groups and for the perchlorate oxygen atoms. This may indicate disorder in the crystal; however, a disordered model could not be derived from the difference Fourier maps calculated. All non-hydrogen atoms were anisotropically refined, the refinement at this point converging at $R = 0.073$, $R_w = 0.070$, and $s = 3.13$. As the crystal is chiral, all coordinates were inverted, $1 - x$, $1 - y$, and $1 - z$, and the parameters were again refined to convergence. The agreement factors now obtained were $R = 0.071$, $R_w = 0.067$, and $s = 3.02$, suggesting that the last choice is the correct one. Hydrogen atoms could not be located in a difference Fourier map, but positions were calculated on the basis of an idealized geometry (C–H = 0.98 Å). In the final cycles non-hydrogen atoms were refined while hydrogen atoms were adjusted according to the movement of the atom to which they are bonded. An extinction parameter was also refined. Data set HT 1 converged at $R = 0.058$, $R_w = 0.050$, and $s = 2.20$. Despite the lower temperature used for HT 2, the refinement converged at a somewhat higher R value (0.070), and standard deviations in bond distances and angles are higher than those obtained for HT 1. No significant differences were found in the two HT structures. In the following only results from HT 1 are quoted.

(b) LT Structure. Systematic absences and intensity distribution showed space group $P2_1$. The structure was solved by direct methods and refined by a full-matrix least-squares refinement. Hydrogen atoms were included at calculated positions but were not refined. The chirality was again tested by refining the two enantiomorphs to convergence. An empirical absorption correction was done after the isotropic refinement;[18] in the final cycles non-hydrogen atoms were anisotropically refined, and an extinction parameter was adjusted. Thermal parameters are high for atoms C10, C12, C13, and C14; refinement of a disordered model did not, however, give reasonable bond distances. Refinement of the LT 2 data set (92 K) converged at $R = 0.043$, $R_w = 0.042$, and $s = 1.69$. Refinement of LT 1 (205.5 K) gave $R = 0.043$, $R_w = 0.043$, and $s = 1.93$ and slightly higher standard deviations in coordinates. In the following only results from LT 2 are quoted.

Final atomic parameters for non-hydrogen atoms are listed in Table II. Anisotropic thermal parameters and coordinates of hydrogen atoms are listed in Tables SI and SII, respectively.[34]

Magnetic Measurements. They were carried out with a Faraday type magnetometer equipped with a helium continuous-flow cryostat in the 300–20 K temperature range. Independence of the magnetic susceptibility from the applied magnetic field was checked at room temperature. The diamagnetic correction was estimated as -255×10^{-6} cm^3 mol^{-1}. In a first time, the magnetic susceptibility was measured in the whole temperature range by cooling down at the scan rate of 0.8 K min^{-1}; then the 202–212 K temperature range was reinvestigated by cooling down and warming up at the scan rate of 5 K h^{-1}.

DSC Measurements. The DSC analysis was conducted on a Perkin-Elmer DSC-2C with its low-temperature attachment (cold finger plunging in a liquid-nitrogen bath) and helium as the purge gas. Volatile sample pans were employed. Cooling as well as heating curves were recorded and analyzed with the TADS Perkin-Elmer system. Temperatures and enthalpies were calibrated with a sample of pure cyclohexane by using its melting (279.69 K, 2678 J mol^{-1}) and crystal-to-crystal (186.10 K, 6740 J mol^{-1}) transitions. The values of T are given with a ±0.5 K accuracy and the enthalpies are exact to ±2% when the scan rate is 10 K min^{-1}.

Table III. Bond Lengths (Å) in $[(Cu(petdien))_2(CO_3)](ClO_4)_2$, with Standard Deviations As Estimated from the Inverse Least-Squares Matrix in Parentheses

bonds	modification	
	HT (294 K)	LT (92 K)
Cu1–O1	2.305 (6)	2.274 (3)
Cu1–O2	1.946 (5)	1.975 (3)
Cu1–N1/Cu1–N1A[a]	2.065 (6)	2.096 (4)/2.049 (4)
Cu1–N2	1.998 (8)	2.003 (4)
Cu2–O1	2.346 (5)	2.254 (3)
Cu2–O3	1.954 (5)	1.979 (3)
Cu2–N3/Cu2–N3A	2.072 (2)	2.072 (3)/2.108 (4)
Cu2–N4	1.980 (8)	2.002 (4)
O1–C1	1.285 (9)	1.290 (5)
O2–C1	1.270 (9)	1.274 (5)
O3–C1	1.289 (9)	1.282 (5)
N1–C2/N1A–C2A	1.518 (15)	1.502 (6)/1.493 (6)
N1–C4/N1A–C4A	1.460 (10)	1.492 (6)/1.513 (7)
N1–C6/N1A–C6A	1.55 (2)	1.503 (7)/1.481 (7)
N2–C3/N2–C3A	1.440 (12)	1.485 (6)/1.509 (6)
N2–C8	1.481 (14)	1.485 (6)
N3–C10/N3A–C10A	1.482 (11)	1.393 (8)/1.482 (6)
N3–C12/N3A–C12A	1.431 (11)	1.444 (8)/1.497 (6)
N3–C14/N3A–C14A	1.456 (10)	1.422 (7)/1.492 (6)
N4–C11/N4–C11A	1.449 (12)	1.492 (6)/1.491 (7)
N4–C16	1.526 (12)	1.489 (5)
C2–C3/C2A–C3A	1.27 (2)	1.513 (7)/1.520 (7)
C4–C5/C4A–C5A	1.502 (10)	1.521 (6)/1.520 (7)
C6–C7/C6A–C7A	1.14 (2)	1.507 (7)/1.500 (9)
C8–C9	1.618 (12)	1.510 (6)
C10–C11/C10A–C11A	1.48 (2)	1.371 (10)/1.505 (8)
C12–C13/C12A–C13A	1.547 (12)	1.547 (8)/1.512 (6)
C14–C15/C14A–C15A	1.381 (13)	1.249 (9)/1.512 (7)
C16–C17	1.552 (13)	1.518 (7)
Cl–O4/ClA–O4A	1.344 (6)	1.428 (3)/1.432 (3)
Cl–O5/ClA–O5A	1.321 (9)	1.439 (4)/1.430 (5)
Cl–O6/ClA–O6A	1.257 (6)	1.437 (3)/1.437 (4)
Cl–O7/ClA–O7A	1.341 (10)	1.444 (4)/1.431 (4)

[a] In the HT modification atoms marked A are related to the corresponding unmarked atoms by a mirror plane: $1 - x, y, z$.

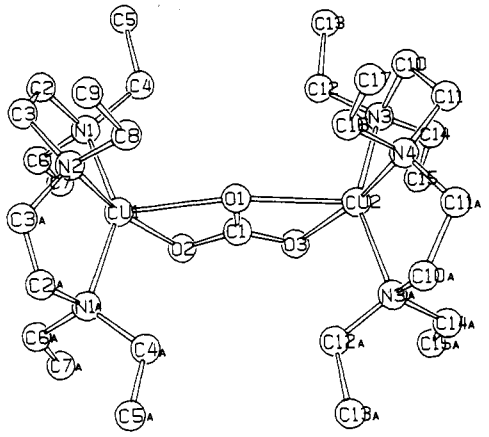

Figure 1. Atomic labeling of the cation. In the HT form there is a crystallographic mirror plane through the bridging group, the copper atoms, and C9, C8, N2, N4, C16, and C17.

Descriptions of the HT and LT Structures

(a) Molecular Geometries in HT and LT Structures. The atomic labeling of the cation is shown in Figure 1. The molecular geometries and the thermal ellipsoids at 294 K (HT 1) and 92 K (LT 2) are depicted in Figure 2. Bond lengths and angles are listed in Tables III and IV, respectively. High thermal parameters, or disorder in the HT form, lead to bond lengths and angles of relatively low accuracy in the perchlorate ion and parts of the petdien groups. Even in the LT form the unresolved disorder causes low accuracy in distances and angles involving C10, C12, C13, C14, and C15.

In both modifications the compound forms dinuclear cations in which the two copper atoms are bridged by a doubly bidentate carbonato group and the petdien groups serve as outer ligands. The perchlorate groups are not coordinated to copper. In the HT form a crystallographic mirror plane passes through the cation, such that the two copper atoms, the carbonato group, and the central nitrogen atoms with the attached ethyl groups are situated on this plane. This symmetry is absent in the LT form. The two copper atoms are crystallographically independent in both forms. Their coordination geometries are similar and may in each case be described in terms of a very distorted trigonal bipyramid in which one carbonato oxygen, O1, and the terminal nitrogen atoms

Table IV. Bond Angles (deg) in $[(Cu(petdien))_2(CO_3)](ClO_4)_2$, with Standard Deviations As Estimated from the Inverse Least-Squares Matrix in Parentheses

angles	modification	
	HT (294 K)	LT (92 K)
O1–Cu1–O2	61.6 (2)	61.9 (1)
O1–Cu1–N1/O1–Cu1–N1A[a]	108.1 (2)	104.7 (1)/111.4 (1)
O1–Cu1–N2	104.9 (4)	103.3 (2)
O2–Cu1–N1/O2–Cu1–N1A	98.2 (2)	101.2 (1)/95.0 (1)
O2–Cu1–N2	166.5 (4)	164.4 (2)
N1–Cu1–N1A	143.7 (4)	143.9 (2)
N1–Cu1–N2/N1A–Cu1–N2	85.7 (2)	86.7 (2)/85.7 (2)
O1–Cu2–O3	61.1 (2)	62.7 (1)
O1–Cu2–N3/O1–Cu2–N3A	106.3 (2)	108.6 (1)/107.6 (1)
O1–Cu2–N4	107.2 (3)	102.4 (1)
O3–Cu2–N3/O3–Cu2–N3A	97.1 (2)	95.4 (2)/99.1 (1)
O3–Cu2–N4	168.2 (3)	165.0 (1)
N3–Cu2–N3A	147.3 (4)	143.8 (2)
N3–Cu2–N4/N3A–Cu2–N4	86.0 (2)	87.2 (2)/87.2 (2)
Cu1–O1–Cu2	163.0 (3)	165.8 (1)
Cu1–O1–C1	81.5 (5)	82.9 (3)
Cu2–O1–C1	81.5 (5)	82.9 (3)
Cu1–O2–C1	98.0 (5)	96.7 (3)
Cu2–O3–C1	99.0 (5)	95.3 (3)
Cu1–N1–C2/Cu1–N1A–C2A	103.4 (7)	105.4 (3)/103.4 (3)
Cu1–N1–C4/Cu1–N1A–C4A	113.4 (5)	113.0 (3)/105.8 (3)
Cu1–N1–C6/Cu1–N1A–C6A	105.4 (6)	108.2 (3)/115.2 (4)
C2–N1–C4/C2A–N1A–C4A	106.1 (8)	109.0 (4)/112.2 (4)
C2–N1–C6/C2A–N1A–C6A	106 (1)	108.6 (4)/112.6 (4)
C4–N1–C6/C4A–N1A–C6A	120.6 (8)	112.4 (4)/107.6 (4)
Cu1–N2–C3/Cu1–N2–C3A	106.5 (6)	104.3 (3)/110.0 (3)
Cu1–N2–C8	107.9 (7)	107.9 (3)
C3–N2–C3A	104 (2)	110.5 (4)
C3–N2–C8	115.5 (7)	112.9 (4)
Cu2–N3–C10/Cu2–N3A–C10A	105.2 (6)	104.5 (4)/103.7 (3)
Cu2–N3–C12/Cu2–N3A–C12A	110.0 (5)	108.1 (3)/108.5 (3)
Cu2–N3–C14/Cu2–N3A–C14A	109.6 (6)	114.2 (3)/111.5 (3)
C10–N3–C12/C10A–N3A–C12A	105.1 (8)	110.3 (7)/110.3 (4)
C10–N3–C14/C10A–N3A–C14A	109.4 (8)	109.5 (9)/108.7 (4)
C12–N3–C14/C12A–N3A–C14A	116.9 (9)	110.1 (9)/113.7 (4)
Cu2–N4–C11/Cu2–N4–C11A	108.4 (6)	107.5 (3)/103.0 (3)
Cu2–N4–C16	109.1 (6)	111.7 (3)
C11–N4–C11A	106 (1)	112.4 (5)
C11–N4–C16/C11A–N4–C16	112.5 (6)	109.7 (4)/112.2 (4)
O1–C1–O2	118.8 (8)	118.3 (4)
O1–C1–O3	118.4 (7)	118.9 (4)
O2–C1–O3	122.8 (8)	122.7 (4)
N1–C2–C3/N1A–C2A–C3A	119.1 (1)	110.2 (4)/108.7 (4)
N2–C3–C2/N2–C3A–C2A	118 (1)	109.5 (4)/107.8 (4)
N1–C4–C5/N1A–C4A–C5A	120.0 (8)	115.5 (4)/116.2 (5)
N1–C6–C7/N1A–C6A–C7A	118 (2)	114.3 (4)/114.0 (4)
N2–C8–C9	109.3 (9)	114.8 (4)
N3–C10–C11/N3A–C10A–C11A	111.3 (9)	123.7 (6)/110.1 (4)
N4–C11–C10/N4–C11A–C10A	109.9 (8)	115.3 (5)/108.3 (4)
N3–C12–C13/N3A–C12A–C13A	117.6 (9)	115.8 (6)/115.7 (5)
N3–C14–C15/N3A–C14A–C15A	120.5 (9)	137.3 (9)/112.4 (4)
N4–C16–C17	120.5 (7)	115.2 (4)
O4–Cl–O5/O4A–ClA–O5A	111.2 (6)	109.3 (2)/110.4 (3)
O4–Cl–O6/O4A–ClA–O6A	113.3 (6)	109.6 (2)/109.7 (3)
O4–Cl–O7/O4A–ClA–O7A	107.7 (5)	109.7 (2)/109.1 (2)
O5–Cl–O6/O5A–ClA–O6A	108.3 (7)	109.3 (2)/108.4 (3)
O5–Cl–O7/O5A–ClA–O7A	105.6 (8)	109.4 (2)/108.7 (3)
O6–Cl–O7/O6A–ClA–O7A	110.4 (8)	109.5 (2)/110.5 (3)

[a] In the HT modification atoms marked A are related to the corresponding unmarked atoms by a mirror plane: $1 - x, y, z$.

Table V. Cell Dimensions As Measured at Various Temperatures[a]

	HT modification, $Cmc2_1$			LT modification, $P2_1$		
T, K	294	252	209.5	205.5	178.5	92
a_o, Å	18.610 (3)	18.483 (8)	18.322 (7)			
b_o, Å	15.449 (3)	15.472 (3)	15.561 (8)			
c_o, Å	14.499 (7)	14.416 (2)	14.232 (9)			
a_m, Å	12.093	12.052	12.019	12.067 (8)	12.066 (2)	12.037 (1)
b_m, Å	14.499	14.416	14.232	13.466 (5)	13.336 (2)	13.145 (3)
c_m, Å	12.093	12.052	12.019	12.474 (6)	12.518 (2)	12.519 (2)
β_m, deg	100.58	100.14	99.31	97.29 (5)	97.15 (1)	96.85 (1)
cryst no.	1	2	2	3	4	4

[a] For the high-temperature modification, dimensions transformed to the monoclinic cell are also given.

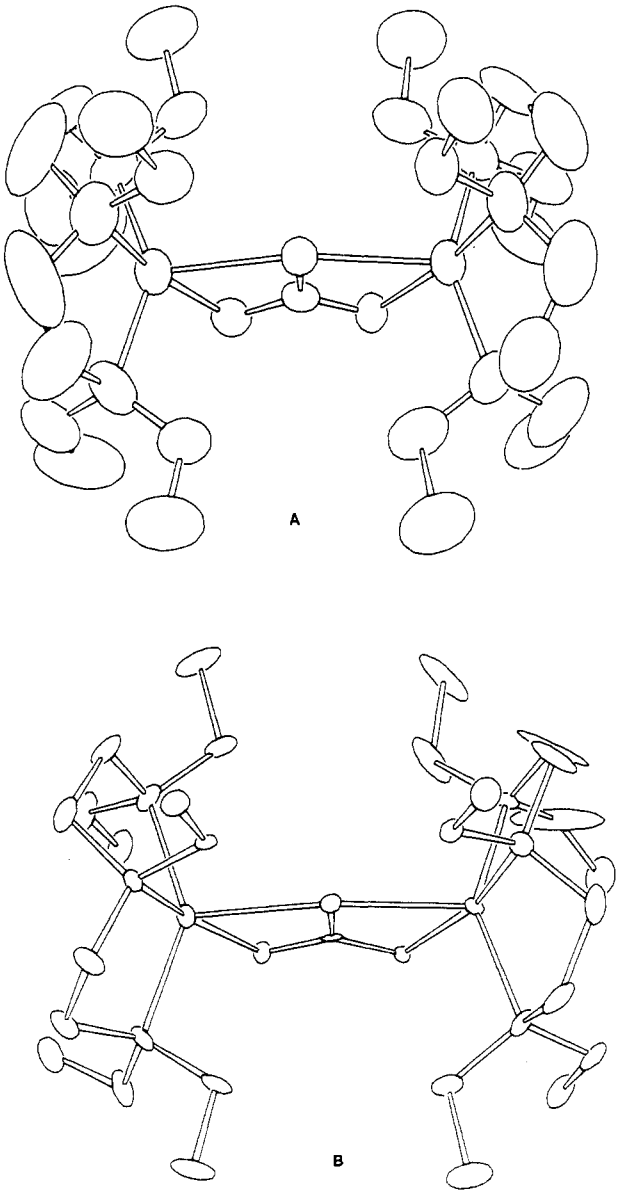

Figure 2. Cation geometry and thermal ellipsoids at the 30% probability level: (A) HT modification; (B) LT modification.

of the petdien group form the equatorial plane, another carbonato oxygen and the central petdien nitrogen being situated in axial positions. The carbonato bridge deviates only slightly from twofold symmetry in both forms. In passing from HT 1 to LT 2, the Cu1–O1 and Cu2–O1 distances decrease and become more equal and the Cu1–O1–Cu2 angle increases from 163.0 to 165.8°. The intramolecular Cu1···Cu2 separation has been changed from 4.601 to 4.494 Å. When the mirror symmetry is removed, the pair of distances Cu1–N1/Cu1–N1A and the pair Cu2–N3/Cu2–N3A

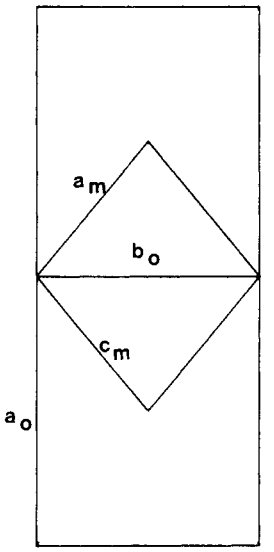

Figure 3. Relation between unit cells of HT and LT modifications.

split and become significantly different, the average bond length being slightly longer than that in the HT form. Also the axial bond lengths Cu1–O2, Cu1–N2, Cu2–O3, and Cu2–N4 increase. Thus, while the Cu1–O1–Cu2 bridge is shortened, the remaining Cu–X bonds on the average become longer at the transition from the HT to the LT form.

(b) Crystal Packing in HT and LT Form. The relationship between the *C*-centered orthorhombic cell of the HT form and the primitive monoclinic cell of the LT form is shown in Figure 3; the unit cell transformation being

$$a_m = \frac{-a_o + b_o}{2} \qquad b_m = c_o \qquad c_m = \frac{a_o + b_o}{2}$$

As the crystal passes through the phase transition, the mirror normal to a_o is broken, giving different lengths for the monoclinic a and c axes and an appreciable lengthening of the latter as compared to half the orthorhombic ab diagonal: $(a + b)/2 = 12.019$ Å at 209.5 K and $c_m = 12.474$ Å at 205.5 K. The twofold screw axis at the same time shortens considerably: $c_o = 14.232$ Å at 209.5 K while $b_m = 13.466$ Å at 205.5 K (see Table V). These are the predominant changes in the cell at the transition. Although the lower symmetry requirement in the monoclinic cell allows a denser packing in the b_m direction, the volume decrease from the HT to the LT form is small due to the increase in c_m. Figure 4 shows a plot of the variation in cell volume with temperature. The volume change at the phase transition is less than 1%.

In Figure S1, projections down the twofold screw axes are compared and in Figure 5, the change in packing along these axes is illustrated. With the *m* symmetry restriction gone, the ethyl groups in the LT modification may twist differently (see, e.g., C6A and C7A in Figure 2). This apparently allows a more dense packing along the 2_1 axis direction. The shortest intermolecular metal-metal separations in the HT form are Cu1···Cu2 (1 − x,

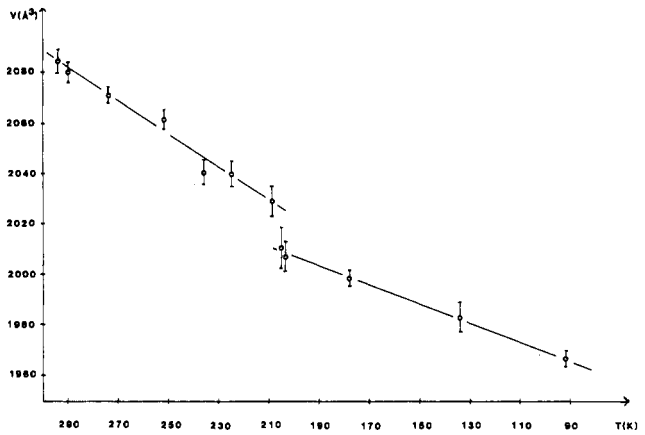

Figure 4. Unit cell volume vs temperature. For the HT form $v_0/2$ is plotted. $3\sigma_v$ is indicated for each point.

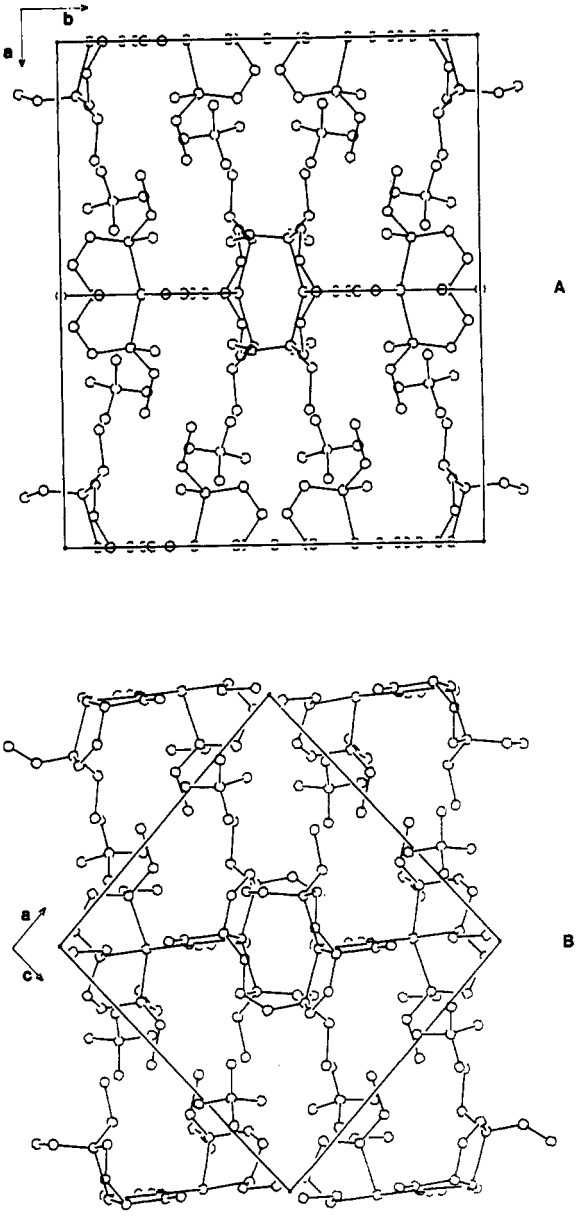

Figure 5. Change of packing in the direction of the screw axis. In part A the HT form is plotted with the *b* axis horizontal. To facilitate comparison between the two structures, the LT form (B) has been plotted with the $a + c$ diagonal running horizontally.

$1 - y, -^1/_2 + z$) of 7.376 Å, Cu2···Cu2 ($1 - x, 1 - y, \pm^1/_2 + z$) of 7.641 Å, and Cu1···Cu1 ($1 - x, -y, \pm^1/_2 + z$) of 9.361 Å, all

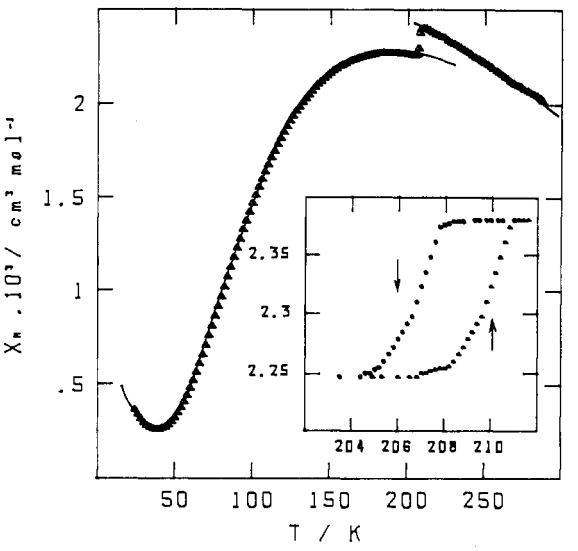

Figure 6. Experimental (Δ) and calculated (—) temperature dependences of χ_M. Inset: variation of χ_M in the 202–212 K temperature range upon cooling down and warming up at scan rate of 5 K h^{-1}.

occurring between molecules situated on the same mirror plane. In the LT form the corresponding metal-metal distances are Cu1···Cu2 ($1 - x, -^1/_2 + y, 1 - z$) of 7.379 Å, Cu2···Cu2 ($1 - x, \pm^1/_2 + y, 1 - z$) of 7.201 Å, and Cu1···Cu1 ($-x, \pm^1/_2 + y, -z$) of 9.228 Å.

Magnetic and Calorimetric Properties

The temperature dependence of the molar magnetic susceptibility χ_M is shown in Figure 6. At room temperature, χ_M is equal to 2.015 (15) × 10^{-3} cm^3 mol^{-1}, which is much below what would be expected for two noninteracting copper(II) ions. Upon cooling down, χ_M smoothly increases and reaches 2.400 (15) × 10^{-3} cm^3 mol^{-1} at 208 K. A sudden break in the χ_M versus T plot then occurs, and at 204 K, χ_M is equal to 2.255 (15) × 10^{-3} cm^3 mol^{-1}. Below 204 K, χ_M exhibits the characteristic behavior of an antiferromagnetically coupled copper(II) dinuclear compound, with a rounded maximum around 190 K and a weakly pronounced Curie tail in the low-temperature range. Around 40 K, χ_M presents a minimum with a very weak value, namely 0.26 (1) × 10^{-3} cm^3 mol^{-1}. The magnetic data confirm that a phase transition takes place around 208 K.

Below 204 K, the magnetic data closely follow the theoretical expression of the magnetic susceptibility for a copper(II) pair

$$\chi_M = \frac{2N\beta^2g^2}{kT}[3 + \exp(-J/kT)]^{-1}(1 - \rho) + \frac{N\beta^2g^2}{2kT}\rho \quad (1)$$

in which the second term accounts for a small proportion ρ of uncoupled copper(II). J is the singlet–triplet (S–T) energy gap, and the other parameters have their usual meaning. The minimization of

$$R = \Sigma(\chi_M^{calcd} - \chi_M^{obsd})^2/\Sigma(\chi_M^{obsd})^2$$

leads to J = −215 (1) cm^{-1}, g = 2.13 (1), and ρ = 0.0101 (2). R is then equal to 2.4 × 10^{-5}, which corresponds to an excellent agreement.

Above 212 K, the magnetic data were fitted with the same expression, eq 1, in which only J was taken as an adjustable parameter. For g and ρ, the values deduced from the data below 204 K were assumed to be correct. Concerning g, this assumption was supported by the fact that the X-band powder EPR spectra do not show any modification when passing through the transition. J was then found equal to −207 (1) cm^{-1}, with R defined as above equal to 3.3 × 10^{-4}.

To get new insights on the phase transition, we reinvestigated the 202–212 K temperature range by cooling down and heating up at a very small scan rate, namely 5 K h^{-1}. In the cooling mode, the transition starts at 207.8 (2) K and is complete at 204.8 (3) K. In the heating mode, the transition starts at 208.2 (3) K and

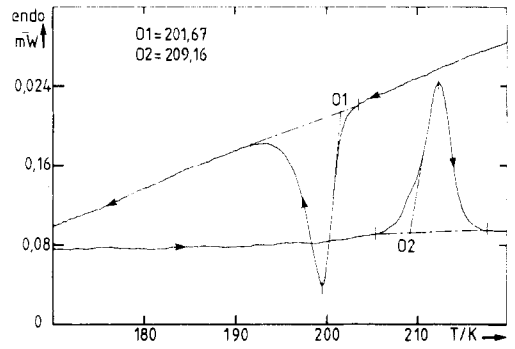

Figure 7. DSC curves at a scan rate of 10 K min^{-1}.

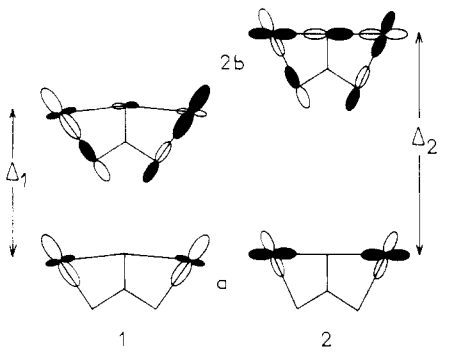

Figure 8. Schematic representation of the singly occupied molecular orbitals in (μ-carbonato)copper(II) dinuclear compounds in cases 1 and 2 (see text).

is complete at 211.0 (3) K. Therefore, from magnetic data, a hysteresis of the order of 3 K is observed.

A typical example of the calorimetric results is given in Figure 7. These results were obtained with a single crystal of 13.11 mg, and the scan rate was ±10 K min^{-1}. There is a very good agreement on the values of ΔH recorded during cooling and heating of the sample. The onset of the transition is found at 201.7 K in the cooling mode and at 209.2 K in the heating mode. The enthalpy variation defined as $H_{HT} - H_{LT}$ is found equal to 3.17 (4) kJ mol^{-1}. The entropy variation is therefore equal to 15.1 (2) J mol^{-1} K^{-1}.

Discussion

The title compound is far from being the first (μ-carbonato)-copper(II) compound. The various modes of coordination of carbonato groups to copper(II) have been summarized by Einstein and Willis,[21] and a review on the chemistry of metal carbonato complexes has been written by Palmer and Eldik.[22] In three already described compounds, the mode of bridging of the carbonato group is similar to that observed in $[(Cu(petdien))_2(CO_3)](ClO_4)_2$. Two of these compounds have been reported to be diamagnetic,[23-25] even at room temperature, which suggests that actually the S–T splitting is larger than, e.g., 800 cm^{-1}. It is therefore interesting to examine the structural differences between those two compounds on the one hand and the title compound on the other hand. Concerning the bridging network, the Cu1–O1 and Cu2–O1 distances are appreciably longer and the deviation from linearity at O1 is somewhat larger in $[(Cu(petdien))_2(CO_3)](ClO_4)_2$ (Cu1–O1 = 2.305 (6) Å, Cu2–O1 = 2.346 (5) Å, Cu1–O1–Cu2 = 163.0 (3)° for the HT modification) than in the two diamagnetic compounds referred to (Cu–O1 = 2.041 (1) Å, Cu–O1–Cu = 176.6 (2)° for one of them;[24,25] Cu–O1 = 2.1527 (4) Å, Cu–O1–Cu = 170.26° for the other one[23]). Also, in those two compounds, the carbonato ligands are equatorially coordinated in a square-pyramidal copper, while here one axial and one equatorial positions in a trigonal-bipyramidal copper are occupied. It is not difficult to understand qualitatively why the antiferromagnetic interaction in our compound (case 1) is significantly less pronounced than in the other two (case 2). In $[(Cu(petdien))_2CO_3](ClO_4)_2$, the interacting magnetic orbitals have a dominant d_{z^2} character due to the trigonal-bipyramidal surroundings.[17] Each magnetic orbital is strongly delocalized toward O2 (or O3) and much more weakly toward O1. In the diamagnetic compounds the interacting magnetic orbitals have a dominant $d_{x^2-y^2}$ character due to the square-pyramidal surroundings. Each of them is equally delocalized toward O1 and O2 (or O3) (we use the labeling scheme of this paper). Since the Cu1–O1–Cu2 pathway is obviously the most efficient to transmit the antiferromagnetic interaction, the S–T splitting is larger in case 2 than in case 1. Another way to account for the differences of magnetic properties consists in saying that from the highest occupied molecular orbital of CO_3^{2-} transforming as a_2'' in D_{3h} symmetry[26] and the two singly occupied metal orbitals, one can construct three molecular orbitals (MO's). If we assume that for both cases 1 and 2, we have a twofold axis collinear with C1–O1, two MO's are antisymmetric with regard to this axis, one being bonding (1b) and the other one antibonding (2b), and one MO is antisymmetric and essentially nonbonding (a). We define the energy gap between the singly occupied 2b and a MO's in the triplet state by Δ_1 in case 1 and Δ_2 in case 2. It is well established that at the first order the magnitude of the antiferromagnetic interaction is proportional to Δ_i^2, $i = 1$ or 2.[17,27] Due to the strong antibonding contribution of the 2p orbital centered on O1 in case 2, the 2b MO in that case is strongly destabilized and Δ_2 is larger than Δ_1, as schematized in Figure 8.

The third (μ-carbonato)copper(II) compound with the same kind of bridge is $[(Cu(teen)Cl)_2(CO_3)]$ with teen = *N,N,N',N'*-tetraethylethylenediamine. In that case, the bridge is strongly asymmetric with Cu1–O1 = 2.093 (2) Å and Cu2–O1 = 2.412 (2) Å. This compound is not diamagnetic but its magnetic properties have not been investigated in detail.[33]

It is worth mentioning here that the compounds in which the carbonato group bridges copper(II) ions either in a bis bidentate fashion with the third oxygen atom noncoordinated, or in a tris monodentate fashion have been reported to be ferromagnetically coupled.[28-30]

When the phase transition takes place, the S–T energy gap suddenly changes from −207 cm^{-1} for the HT modification to −215 cm^{-1} for the LT modification. Again, this slight variation in the magnitude of the interaction can be easily understood. In the LT phase, the Cu1–O1–Cu2 linkage is more linear (Cu1–O1–Cu2 = 165.8 (1)° in the LT phase and 163.0 (3)° in the HT phase) and the Cu1–O1 and Cu2–O1 distances are shorter (2.274 (3) and 2.254 (3) Å in the LT phase, and 2.305 (4) and 2.346 (5) Å in the HT phase), which increases the antibonding character of the 2b MO. In fact, when all the variations of bond lengths and angles around the copper atoms associated with the phase transition are carefully examined, one can see that the trigonal-bipyramidal character is more pronounced in the HT phase or if one prefers, that the admixture of $d_{x^2-y^2}$ metal orbital in the

(21) Einstein, F. W. B.; Willis, A. C. *Inorg. Chem.* **1981**, *20*, 609.
(22) Palmer, D. A.; Van Eldik, R. *Chem. Rev.* **1983**, *83*, 651.
(23) Churchill, M. R.; Davies, G.; El-Sayed, M.; El-Shazly, M.; Hutchinson, J. P.; Rupich, M. W.; Watkins, K. O. *Inorg. Chem.* **1979**, *18*, 2296.
(24) Davis, A. R.; Einstein, F. W. B.; Curties, N. F.; Martin, J. W. L. *J. Am. Chem. Soc.* **1978**, *100*, 6258.
(25) Davis, A. R.; Einstein, F. W. B. *Inorg. Chem.* **1980**, *19*, 1203.
(26) Connor, J. A.; Hillier, I. H.; Saunders, V. R.; Barber, M. *Mol. Phys.* **1972**, *23*, 81.
(27) Hay, P. J.; Thibeault, J. C.; Hoffmann, R. *J. Am. Chem. Soc.* **1975**, *97*, 4884.
(28) Gregson, A. K.; Healy, P. C. *Inorg. Chem.* **1978**, *17*, 2969.
(29) Gregson, A. K.; Moxon, T. N. *Inorg. Chem.* **1981**, *20*, 78; **1982**, *21*, 3464.
(30) Kolks, G.; Lippard, S. J.; Waszczak, J. V. *J. Am. Chem. Soc.* **1980**, *102*, 4833.
(31) Cartier, C.; Thuery, P.; Verdaguer, M.; Zarembowitch, J.; Michalowicz, A. *J. Phys. (Les Ulis, Fr.)* **1986**, *47*, C8-563.
(32) Zarembowitch, J.; Thuery, P.; Dworkin, A.; Michalowicz, A. *J. Chem. Res. Synop.* **1987**, 146.
(33) Churchill, M. R.; Davis, G.; El-Sayed, M. A.; El-Shazly, M. F.; Hutchinson, J. P.; Rupich, M. W. *Inorg. Chem.* **1980**, *19*, 201.
(34) See paragraph at end of paper regarding supplementary material.

description of the ground state is more important in the LT phase. Such a subtle effect explains the abrupt break in the magnetic susceptibility curve around 208 K upon cooling down.

The most thoroughly studied phase transitions in molecular inorganic chemistry are certainly those concerning the spin-crossover complexes.[13-15] In that case, however, the transition is driven by the intraionic electron transfer, which modifies the occupancy of the metal orbitals, and hence the electronic content of the metal-ligand bonds. When a single electron is involved in this intraionic transfer [Co(II)], the average variation of metal-ligand bond lengths is around 0.1 Å and when two electrons are involved, this variation is in the range 0.12-0.15 Å for Fe(III) and 0.14-0.24 Å for Fe(II).[13,15,31] In the present case, the phase transition is not related to an electronic instability, and on average, there is no variation of the metal-ligand bond lengths. However, the enthalpy and entropy variations associated with the transition are rather important; they are of the same order of magnitude as those in spin-crossover compounds.[13,32] Concerning the entropy variation ΔS, it is usual to write

$$\Delta S = \Delta S_{el} + \Delta S_{vib,intra} + \Delta S_{vib,inter} \quad (2)$$

In the present case, it is clear that ΔS_{el} is almost negligible since the only electronic effect of the transition is to increase the S-T energy gap in absolute value from 207 to 215 cm^{-1}. $\Delta S_{vib,intra}$ may also be expected to be rather small since the intramolecular geometry is weakly modified. It follows that the lattice term $\Delta S_{vib,inter}$ would be predominant.

Registry No. $[(Cu(petdien))_2(CO_3)](ClO_4)_2$, 111959-29-6.

Supplementary Material Available: Listings of anisotropic thermal parameters (Table SI) and coordinates of hydrogen atoms (Table SII) in HT (a) and LT (b) forms and a drawing of the crystal packing as projected down the screw axis in HT (A) and LT (B) forms (Figure S1) (6 pages); tables of calculated and observed structure factors (27 pages). Ordering information is given on any current masthead page.

Contribution from the Department of Chemistry, Northwestern University, Evanston, Illinois 60208

Synthesis and Characterization of $Na_2Ti_2Se_8$, a New One-Dimensional Solid-State Polyselenide

Doris Kang and James A. Ibers*

Received July 30, 1987

The compound $Na_2Ti_2Se_8$ has been prepared through the reaction of Ti metal with a Na_2Se/Se flux at 345 °C. The compound crystallizes with four formula units in space group C_{2h}^5-$P2_1/c$ of the monoclinic system in a cell of dimensions a = 12.841 (7) Å, b = 7.146 (4) Å, c = 12.994 (8) Å, β = 106.18 (2)° at −160 °C. The structure contains infinite, one-dimensional Ti/Se chains that run parallel to the c axis. In these chains the Ti centers are seven-coordinate. These chains are isolated from one another by Na^+ ions. When the Se-Se bonds are taken into account, the composition of the chain is $^1_\infty[Ti_2(Se_2)_3(Se)_2^{2-}]$ and the compound contains Ti^{4+}.

Introduction

Molten alkali-metal polysulfides have been used intermittently as fluxes in the crystal growth of solid-state sulfides.[1] Previous reports have involved syntheses at high temperatures (>800 °C) and appear not to have yielded solid-state polysulfides.[1-3] Recently,[4] we found that the addition of transition metals to alkali-metal polysulfides at low temperatures (300-400 °C) affords new solid-state polysulfides, typified by $K_4Ti_3Si_{14}$, in which there occur chains of $^1_\infty[Ti_3(S_2)_6(S)_2^{4-}]$, that is, infinite one-dimensional chains composed of Ti^{4+} centers bonded to S_2^{2-} and S^{2-} species. This compound is the first member of an entirely new series of one-dimensional solid-state polysulfides.

Because low-dimensional materials are of wide interest,[5] we are engaged in extending this type of synthesis to other metals and other chalcogens. Here we present the synthesis and characterization of $Na_2Ti_2Se_8$, the first member of related series of one-dimensional polyselenides.

Experimental Section

$Na_2Ti_2Se_8$. A 0.048-g (0.38-mmol) sample of anhydrous Na_2Se (Alfa, 95%), 0.0090 g (0.19 mmol) of Ti metal powder (Aesar, 99.9%), and 0.152 g (1.9 mmol) of Se powder (Atomergic, 99.999%) were combined in a silica tube that was subsequently evacuated to ~10^{-5} Torr. The mixture was heated to 345 °C and kept there for 100 h before being cooled to room temperature at 3 °C/h. The resultant material was washed with water to remove excess sodium polyselenides. The yield of purple-brown, slightly air-sensitive crystals of $Na_2Ti_2Se_8$ was approximately 18% based on the initial titanium present. The presence of Ti and Se was established by microprobe analysis (EDAX) of single crystals. The composition of the material was established from an X-ray structure determination.

X-ray Structure Analysis. A suitable crystal was mounted directly in the cold stream of an Enraf Nonius CAD4 diffractometer. Crystal data and experimental details are given in Table I. The six standards from diverse regions of reciprocal space that were monitored every 3 h during data collection remained constant within counting statistics.

The structure was solved through a combination of Patterson and direct methods. A successful trial structure was difficult to find owing to a lack of knowledge of the composition of the material and reluctance to accept what turned out to be the correct solution for the Se positions. The structure was refined in a straightforward manner. The model was restricted to isotropic motion because the thermal parameters are very small for this low-temperature data set and because we felt that the magnitude of the absorption correction would render any anisotropic thermal parameters suspect. The final refinement was carried out on F_o^2, use being made of all unique data including those for which $F_o^2 \leq 0$. The peaks on a final difference electron density synthesis ranged from +3.5 to −3.8 e/Å^3; these heights may be compared with that of about 24 e/Å^3 for a Na atom in the structure. An analysis of $\sum w(F_o^2 - F_c^2)^2$ as a function of F_o^2, Miller indices, and setting angles displayed no unexpected trends. There is no evidence of nonstoichiometry or of oxygen contamination. Table II presents the final positional and isotropic thermal parameters while Table SI[6] presents a list of $10|F_o|$, $10|F_c|$, and $\sigma(F_o^2)$.

(1) Scheel, H. J. *J. Cryst. Growth* **1974**, *24*, 669-673 and references therein.
(2) Bronger, W.; Günther, O. *J. Less*-Common *Met.* **1972**, *27*, 73-79.
(3) Huster, J.; Bronger, W. *Z. Naturforsch., Anorg. Chem., Org. Chem.* **1974**, *29B*, 594-595.
(4) Sunshine, S. A.; Kang, D.; Ibers, J. A. *J. Am. Chem. Soc.* **1987**, *109*, 6202-6204.
(5) As an example, see: *Electron Properties of Inorganic Quasi-One-Dimensional Compounds*; Monceau, P., E.; Reidel: Dordrecht, The Netherlands, 1985.

(6) Supplementary material.

0020-1669/88/1327-0549$01.50/0